

processing. In one case, spikes from a putative interneuron and a putative pyramidal cell were recorded simultaneously and, after labelling, a parvalbumin-positive basket cell and a pyramidal cell were recovered. The interneuron was more strongly modulated by the current steps and was also more strongly labelled than the pyramidal cell.

Anatomical and immunohistochemical visualization

The rats were perfused with fixative 4 h after labelling. Immunofluorescence and peroxidase reactions for light microscopy and electron microscopy were performed as described previously^{18,29}. Antibodies against parvalbumin, CCK, somatostatin and mGluR7a were gifts from K. Baimbridge, A. Varro, A. Buchan and R. Shigemoto, respectively; antibodies against mGluR1 were obtained from DiaSorin. The specificity of these antibodies is discussed elsewhere²⁹.

Data analysis

The LFP were detected by calculating the theta (3–6 Hz) to delta (2–3 Hz) frequency power ratio in 2-s windows of the LFP⁵. A ratio greater than four in at least three consecutive windows marked theta episodes, and a ratio less than two in at least three consecutive windows indicated epochs that are called non-theta/non-sharp-wave periods, which lacked field ripples. Non-theta/non-sharp-wave periods contained oscillations of 1 Hz and/or 2–3 Hz, but were not further analysed in this study, owing to the larger variability in cell activity. To determine the phase relationship between single-cell and theta activity, the troughs of the theta oscillations were detected in the filtered signal (3–6 Hz). Each spike was assigned to a given phase (bin size 20°) between the troughs (0° and 360°) and all theta cycles were superimposed⁵. Theta phase was analysed using circular statistics³⁰.

The LFP was filtered at 90–140 Hz for the detection of sharp-wave-associated ripples and the power (r.m.s. amplitude) of the filtered signal was calculated in 10-ms windows⁵. The threshold for ripple detection was set to 5 s.d. above the mean power. The beginning and the end of the sharp wave were set where the power crossed 1 s.d. above the mean power. The maximum amplitude of the oscillation was detected by a peak-finding algorithm. To evaluate the firing pattern of a single neuron during sharp waves, ripple episodes were normalized. Because sharp waves are often not symmetrical, the periods between the beginning and the ripple maximum, and the ripple maximum and the end of the sharp-wave episodes were each divided into four bins, and spikes were sorted into bins. To test whether potential correlations of firing patterns with sharp waves arose by chance, for each cell the exact number and duration of observed sharp-wave windows were randomly shuffled over the period of non-theta/non-sharp-wave epoch, and the spikes detected in the windows were binned. A neuron was considered to be a 'single peak' cell if the number of spikes in six bins surrounding the ripple maximum was higher in the observed sharp-wave correlogram than the mean + 2 s.d. from 100 shuffled correlograms. For anti-sharp-wave cells the number of spikes in six bins surrounding the ripple maximum was lower in the observed sharp wave correlogram than the mean – 2 s.d. from 100 shuffled correlograms. For biphasic neurons, the number of spikes in four bins surrounding the beginning of the sharp wave was higher in the observed sharp-wave correlogram than the mean + 1 s.d. from 100 shuffled correlograms, and the number of spikes in ten consecutive bins, starting from the fourth bin of the sharp wave, was lower in the observed sharp waves than the mean – 2 s.d. of the respective bins from 100 shuffled correlograms. The discharge frequency of single cells during three different brain states (theta, sharp-wave and non-theta/non-sharp-wave) was calculated by dividing the number of spikes with the summed duration of the respective brain state.

Received 15 October; accepted 29 November 2002; doi:10.1038/nature01374.

- O'Keefe, J. & Nadel, L. *The Hippocampus as a Cognitive Map* (Clarendon, Oxford, UK, 1978).
- Fox, S. E. Membrane potential and impedance changes in hippocampal pyramidal cells during theta rhythm. *Exp. Brain Res.* **77**, 283–294 (1989).
- Ylinen, A. *et al.* Sharp wave-associated high-frequency oscillation (200 Hz) in the intact hippocampus: Network and intracellular mechanisms. *J. Neurosci.* **15**, 30–46 (1995).
- Ylinen, A. *et al.* Intracellular correlates of hippocampal theta rhythm in identified pyramidal cells, granule cells, and basket cells. *Hippocampus* **5**, 78–90 (1995).
- Csicsvari, J., Hirase, H., Czurko, A., Mamiya, A. & Buzsáki, G. Oscillatory coupling of hippocampal pyramidal cells and interneurons in the behaving rat. *J. Neurosci.* **19**, 274–287 (1999).
- Buzsáki, G. Theta oscillations in the hippocampus. *Neuron* **33**, 325–340 (2002).
- Cobb, S. R., Buhl, E. H., Halasy, K., Paulsen, O. & Somogyi, P. Synchronization of neuronal activity in hippocampus by individual GABAergic interneurons. *Nature* **378**, 75–78 (1995).
- Freund, T. F. & Buzsáki, G. Interneurons of the hippocampus. *Hippocampus* **6**, 347–470 (1996).
- Fricker, D. & Miles, R. Interneurons, spike timing, and perception. *Neuron* **32**, 771–774 (2001).
- McBain, C. J. & Fisahn, A. Interneurons unbound. *Nature Rev. Neurosci.* **2**, 11–23 (2001).
- Buhl, E. H., Halasy, K. & Somogyi, P. Diverse sources of hippocampal unitary inhibitory postsynaptic potentials and the number of synaptic release sites. *Nature* **368**, 823–828 (1994).
- Traub, R. D. *et al.* Axonal gap junctions between principal neurons: A novel source of network oscillations, and perhaps epileptogenesis. *Rev. Neurosci.* **13**, 1–30 (2002).
- Vanderwolf, C. H. Cerebral activity and behavior: Control by central cholinergic and serotonergic systems. *Int. Rev. Neurobiol.* **30**, 225–340 (1988).
- Pinault, D. A novel single-cell staining procedure performed *in vivo* under electrophysiological control: Morpho-functional features of juxtacellularly labeled thalamic cells and other central neurons with biocytin or neurobiotin. *J. Neurosci. Methods* **65**, 113–136 (1996).
- McBain, C. J., DiChiara, T. J. & Kauer, J. A. Activation of metabotropic glutamate receptors differentially affects two classes of hippocampal interneurons and potentiates excitatory synaptic transmission. *J. Neurosci.* **14**, 4433–4445 (1994).
- Sik, A., Penttonen, M., Ylinen, A. & Buzsáki, G. Hippocampal CA1 interneurons: An *in vivo* intracellular labeling study. *J. Neurosci.* **15**, 6651–6665 (1995).
- Ali, A. B. & Thomson, A. M. Facilitating pyramid to horizontal oriens-alveus interneurone inputs: Dual intracellular recordings in slices of rat hippocampus. *J. Physiol. (Lond.)* **507**, 185–199 (1998).

- Maccaferri, G., Roberts, J. D. B., Szucs, P., Cottingham, C. A. & Somogyi, P. Cell surface domain specific postsynaptic currents evoked by identified GABAergic neurones in rat hippocampus *in vitro*. *J. Physiol. (Lond.)* **524**, 91–116 (2000).
- Nakazawa, K. *et al.* Requirement for hippocampal CA3 NMDA receptors in associative memory recall. *Science* **297**, 211–218 (2002).
- Brun, V. H. *et al.* Place cells and place recognition maintained by direct entorhinal-hippocampal circuitry. *Science* **296**, 2243–2246 (2002).
- Gillies, M. J. *et al.* A model of atropine-resistant theta oscillations in rat hippocampal area CA1. *J. Physiol. (Lond.)* **543**, 779–793 (2002).
- Spruston, N., Schiller, Y., Stuart, G. & Sakmann, B. Activity-dependent action potential invasion and calcium influx into hippocampal CA1 dendrites. *Science* **268**, 297–300 (1995).
- Harris, K. D., Hirase, H., Leinekugel, X., Henze, D. A. & Buzsáki, G. Temporal interaction between single spikes and complex spike bursts in hippocampal pyramidal cells. *Neuron* **32**, 141–149 (2001).
- Skaggs, W. E., McNaughton, B. L., Wilson, M. A. & Barnes, C. A. Theta phase precession in hippocampal neuronal populations and the compression of temporal sequences. *Hippocampus* **6**, 149–172 (1996).
- Mehta, M. R., Lee, A. K. & Wilson, M. A. Role of experience and oscillations in transforming a rate code into a temporal code. *Nature* **417**, 741–746 (2002).
- Harris, K. D. *et al.* Spike train dynamics predicts theta-related phase precession in hippocampal pyramidal cells. *Nature* **417**, 738–741 (2002).
- Katona, I., ACSády, L. & Freund, T. F. Postsynaptic targets of somatostatin-immunoreactive interneurons in the rat hippocampus. *Neuroscience* **88**, 37–55 (1999).
- Magee, J. C. & Johnston, D. A synaptically controlled, associative signal for Hebbian plasticity in hippocampal neurons. *Science* **275**, 209–213 (1997).
- Losonczy, A., Zhang, L., Shigemoto, R., Somogyi, P. & Nusser, Z. Cell type dependence and variability in the short-term plasticity of EPSCs in identified mouse hippocampal interneurons. *J. Physiol. (Lond.)* **542**, 193–210 (2002).
- Zar, J. H. *Biostatistical Analysis* (Prentice Hall, New Jersey, 1999).

Supplementary Information accompanies the paper on Nature's website (<http://www.nature.com/nature>).

Acknowledgements We thank G. Horseman and S. Gray from Cambridge Electronic Design, and P. Jays and L. Norman for technical assistance. We thank Z. Nusser, G. Tamas and J. Csicsvari for critically reading an earlier version of the manuscript, and Y. Dalezios for help with the statistics. T.K. was supported by an Erwin Schroedinger Fellowship from the Austrian Science Fund during part of this study; G.B. was supported by the National Institutes of Health.

Competing interests statement The authors declare that they have no competing financial interests.

Correspondence and requests for materials should be addressed to T.K. (e-mail: thomas.klausberger@pharm.ox.ac.uk).

Yeast genome duplication was followed by asynchronous differentiation of duplicated genes

Rikke B. Langkjær*, Paul F. Cliften†, Mark Johnston† & Jure Piškur*

* BioCentrum-DTU, Technical University of Denmark, Building 301, DK-2800 Lyngby, Denmark

† Department of Genetics and Genome Sequencing Center, Washington University School of Medicine, St. Louis, Missouri 63110, USA

Gene redundancy has been observed in yeast, plant and human genomes, and is thought to be a consequence of whole-genome duplications^{1–3}. Baker's yeast, *Saccharomyces cerevisiae*, contains several hundred duplicated genes¹. Duplication(s) could have occurred before or after a given speciation. To understand the evolution of the yeast genome, we analysed orthologues of some of these genes in several related yeast species. On the basis of the inferred phylogeny of each set of genes, we were able to deduce whether the gene duplicated and/or specialized before or after the divergence of two yeast lineages. Here we show that the gene duplications might have occurred as a single event, and that it probably took place before the *Saccharomyces* and *Kluyveromyces* lineages diverged from each other. Further evolution of each duplicated gene pair—such as specialization or differentiation of

the two copies, or deletion of a single copy—has taken place independently throughout the evolution of these species.

Most genomes show a high degree of redundancy^{4–6}, which can arise from single-gene duplications, duplications of short chromosomal segments or of entire chromosomes, or by duplication of the entire genome. All of these events are believed to play an important part in biological evolution⁷. Two genes derived from a gene duplication are said to be paralogous. One of the paralogues is often subsequently deleted from the genome. Rarely, paralogues are preserved because they differentiate and become functionally specialized. In the fruitfly, the nematode worm and the fission yeast genomes, most paralogous genes are dispersed. In contrast, duplicated genes in the yeast *S. cerevisiae*¹, the plant *Arabidopsis thaliana*², and in humans, *Homo sapiens*³, often occur in large segmental duplications in which members of homologous gene pairs are located in the same order along the two distinct segments and are sporadically interspersed with unique genes.

Owing to its small size, high gene density and a paucity of introns⁸, the *S. cerevisiae* genome is ideal for studying the origins of genome redundancy. Since their discovery^{9,10}, the origin of duplicated blocks of genes in the yeast genome has been controversial. A single genome duplication followed by partial deletions has been proposed as the origin of the duplicated *S. cerevisiae* regions/blocks¹, which consist of 655 duplicated genes¹¹. However, a series of continuous, smaller duplications¹², or a combination of both types of event^{13,14} could result in a similar genome configuration. A recent detailed analysis of the chromosomal gene order in several partially sequenced ascomycetous yeasts¹⁵ showed that three-quarters of the *S. cerevisiae* genome consists of 'sister regions' originating from the ancient duplicated segments¹⁶. The conserva-

tion of transcriptional orientation of duplicated gene pairs with respect to the centromere, the lack of triplicated regions, and pairing of the *S. cerevisiae* centromeres, strongly support the hypothesis of the whole-genome duplication^{1,16}. However, the timing of the whole-genome duplication and the subsequent fate of duplicated genes remain unclear.

We determined, and analysed, the sequence of genes orthologous to some duplicated *S. cerevisiae* genes from several yeast species. These species were selected on the basis of their phylogenetic relationship with *S. cerevisiae* (ref. 17; Fig. 1a). *Saccharomyces bayanus*, a *sensu stricto* species, is one of the closest relatives of *S. cerevisiae*¹⁷. *Saccharomyces castellii*, a *sensu lato* species, branched out before the *S. cerevisiae* and *S. bayanus* lineages separated. These three yeasts can generate respiratory deficient mutants (petite-positive phenotype), can grow anaerobically, and in general possess very similar physiological properties¹⁸. In contrast, *Saccharomyces kluyveri* and *Kluyveromyces lactis* are petite-negative, and have a somewhat different metabolism; *S. kluyveri* can also grow anaerobically, but exhibits weaker glucose repression of the respiratory pathway^{19,20}; *K. lactis* is the least related¹⁷ to *S. cerevisiae*, and can only grow aerobically²¹. *Candida albicans*, the fifth species used in our analysis, is not a very close relative of the other species we analysed¹⁷. Thirty-eight genes, covering almost half of the 52 duplicated blocks in the *S. cerevisiae* genome¹¹ and representing one-tenth of the total number of the *S. cerevisiae* duplicated genes, were analysed for their phylogenetic relationship (Table 1, Fig. 1b). We assumed that only a negligible horizontal transfer of the genetic material has occurred after separation of these yeasts, because, in general, the gene phylogenetic trees recapitulated the species phylogeny.

When a gene from one of the yeast species was compared with the pair of duplicated *S. cerevisiae* genes, two different types of phylogenetic tree could be obtained, depending on whether the *S. cerevisiae* gene pair was duplicated and/or differentiated before or after the species carrying the gene in question separated from the *S. cerevisiae* lineage (Fig. 1b). If a gene grouped with one of the *S. cerevisiae* paralogues (tree type A; Fig. 1b), we inferred that the duplication or gene specialization event in *S. cerevisiae* took place before the separation of the yeast lineages, and therefore this gene is of type A. If a gene was positioned outside the duplicated *S. cerevisiae* gene pair (tree type B; Fig. 1b), we inferred that speciation of the two yeast lineages took place before the gene duplication or specialization event. Surprisingly, all species contained a mixture of A- and B-type genes (Table 1). The proportion of A-type genes decreased as the genetic distance between *S. cerevisiae* and the analysed yeast species became greater, being 95% for *S. bayanus*, 81% for *S. castellii*, 58% for *S. kluyveri*, 28% for *K. lactis* and 3% for *C. albicans*. Apparently, the organization of the duplicated blocks and genes is very similar between *S. cerevisiae* and *S. bayanus*, whereas *C. albicans* seems to be a pre-duplication lineage. The branch-position of a majority of *C. albicans* gene sequences agrees with the phylogenetic relationship among studied yeast species. However, in a few cases (for example, the *GUP* gene) the position is embedded within the tree, suggesting a limited horizontal transfer.

In general, the switch from B type to A type for a certain gene is highly ordered, and the gene status in each species is a function of the phylogenetic relationship among the studied species. In other words, all A-type genes found in *K. lactis* are also of A type in the other yeasts, all of which are more closely related to *S. cerevisiae*; all *S. kluyveri* A-type genes are also of A type in *S. bayanus* and *S. castellii*; and the same rule applies for all *S. castellii* A-type genes. Once a yeast lineage acquired a gene of A type, the nature of this gene was preserved in all descending lineages. In addition, among the duplication blocks, which were represented by more than one gene (block 2, 8, 11, 23, 30, 34, 37, 43, 46 and 54), roughly 40% consisted of an A-type gene and a B-type gene in at least one species. For example, block 23 was represented by two gene pairs,

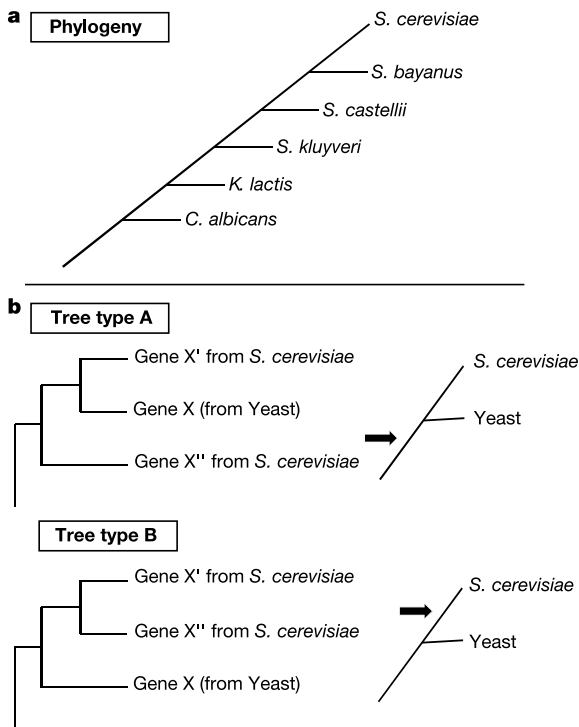


Figure 1 Phylogenetic relationship among different yeasts and among genes homologous to the duplicated *S. cerevisiae* genes. **a**, A schematic phylogenetic tree adapted from ref. 17. **b**, A yeast gene, homologous to the *S. cerevisiae* duplicated gene pair, can either be grouped with one of the duplicated genes (type A), or be outside the duplicated gene pair (type B). In the first case, the duplication or differentiation/specialization took place (see arrow) before the *S. cerevisiae* lineages and the studied yeast separated. In the case of tree type B, the duplication or differentiation/specialization event took place (see arrow) after separation of the lineages.

Table 1 Phylogenetic analysis of genes, homologous to selected *S. cerevisiae* paralogues

Block	<i>S. cerevisiae</i>				Tree type					
	Gene	Systematic	Gene	Systematic	<i>S. b.</i>	<i>S. ca.</i>	<i>S. k.</i>	<i>K. l.</i>	<i>C. a.</i>	
2	<i>MYO4</i>	YAL029C	-	<i>MYO2</i>	YOR326W	A	A	A	-	n.r.
2	<i>CDC19/PYK1</i>	YAL038W	-	<i>PYK2</i>	YOR347C	A	A	A	-	n.r.
3	<i>BAP2</i>	YBR068C	-	<i>BAP3</i>	YDR046C	A	A	B	-	-
8	<i>SMY2</i>	YBR172C	-	<i>YPL105C</i>	YPL105C	A	A	A	B	B
8	<i>SSE2</i>	YBR169C	-	<i>SSE1</i>	YPL106C	A	A	A	-	B
10	<i>PHO87</i>	YCR037C	-	<i>PHO90</i>	YJL198W	A	B	B	-	B
11	<i>CIT2</i>	YCR005C	-	<i>CIT1</i>	YNR001C	A	A	A	A	B*
11	<i>ADY2</i>	YCR010C	-	<i>FUN34</i>	YNR002C	A	A	B	-	B
11	<i>ARE1</i>	YCR048W	-	<i>ARE2</i>	YNR019W	A	A	A	-	B
11	<i>SOL2</i>	YCR073WA	-	<i>SOL1</i>	YNR034W	A	A	A*	-	B
21	<i>SIF2</i>	YDL042C	-	<i>HST1</i>	YOL068C	A	A*	B	B	B
22	<i>AKR1</i>	YDR264C	-	<i>AKR2</i>	YOR034C	A	A	A	A	B
23	<i>EFT2</i>	YDR385W	-	<i>EFT1</i>	YOR133W	B	B	B	-	B
23	<i>PDR15</i>	YDR406W	-	<i>PDR5</i>	YOR153W	A	A	n.r.	B	B
27	<i>RPS24A</i>	YER074W	-	<i>RPS24B</i>	YIL069C	B	B	B	B	B
28	<i>GEA2</i>	YEL022W	-	<i>GEA1</i>	YJR031C	A	A	-	-	B
29	<i>GND2</i>	YGR256W	-	<i>GND1</i>	YHR183W	A	A	-	B	B
30	<i>GSC2/GLS2</i>	YGR032W	-	<i>FKS1/GLS1</i>	YLR342W	A	B*	B*	-	B
30	<i>YGR043C</i>	YGR043C	-	<i>TAL1</i>	YLR354C	A	A	A*	A*	B
33	<i>GUP1</i>	YGL084C	-	<i>GUP2</i>	YPL189W	A	A	A	A	A
34	<i>DBF2</i>	YGR092W	-	<i>DBF20</i>	YPR111W	A	n.r.	B	B	B
34	<i>RPS23A</i>	YGR118W	-	<i>RPS23B</i>	YPR132W	A	B*	B	B	B
37	<i>TOM71/TOM72</i>	YHR117W	-	<i>TOM70</i>	YNL121C	A	A	A	-	B
37	<i>YCK1</i>	YHR135C	-	<i>YCK2</i>	YNL154C	A	A	-	B	B
38	<i>UBP7</i>	YIL156W	-	<i>UBP11</i>	YKR098C	A	A	A	-	B
39	<i>SEC24</i>	YIL109C	-	<i>SFB2</i>	YNL049C	A	A	A	-	B
42	<i>YJR061W</i>	YJR061W	-	<i>MNN4</i>	YKL201C	A	A	B	B	B
43	<i>GFA1</i>	YKL104C	-	<i>YMR085W</i>	YMR085W	A	A	A	-	n.r.
				<i>YMR084W</i>	YMR084W					
43	<i>YKL133C</i>	YKL133C	-	<i>YMR115W</i>	YMR115W	A	A	A	-	B*
45	<i>EXG1</i>	YLR300W	-	<i>SPR1</i>	YOR190W	A	A	A	B	B
46	<i>BUL2</i>	YML111W	-	<i>BUL1</i>	YMR275C	A	A	B	-	B
46	<i>ATR1</i>	YML116W	-	<i>YMR279C</i>	YMR279C	A	A*	A*	-	B
49	<i>CLA4</i>	YNL298W	-	<i>SKM1</i>	YOL113W	A	A	-	-	B
50	<i>YNL108C</i>	YNL108C	-	<i>TFC7</i>	YOR110W	A	A	A	-	B
54	<i>RPL13A</i>	YDL082W	-	<i>RPL13B</i>	YMR142C	A	B	B	B	B
54	<i>RPS16B</i>	YDL083C	-	<i>RPS16A</i>	YMR143W	A	B	B	B	B
Possible	<i>PET9/AAC2</i>	YBL030C	-	<i>AAC3</i>	YBR085W	A	A*	B*	B*	B*
Possible	<i>STP1</i>	YDR463W	-	<i>STP2</i>	YHR006W	A	A	A	-	-

The block numbers, the genes contained within them and the chromosome location can be found at <http://wolfe.gen.tcd.ie> and in ref. 11. For definition of tree type, see Fig. 1b. Further details of the analysis can be found in Methods; further details of the employed sequences, including the accession numbers, and the phylogenetic trees are available as Supplementary Information. Genes, where relevant branches were supported by bootstrap values of at least 750 out of 1,000, were either designated as A or B type, or in the case that the relevant branch was supported by values of 500–749 out of 1,000, as A* or B* type. *S. b.*, *S. bayanus*; *S. ca.*, *S. castellii*; *S. k.*, *S. kluyveri*; *K. l.*, *K. lactis*; *C. a.*, *C. albicans*; n.r., not resolved; -, sequences not available.

EFT1/EFT2 and *PDR15/PDR5*, but these two genes gave different tree types in *S. bayanus* and *S. castellii* (Table 1). Therefore, the fate of the duplicated genes has apparently not been the same, and there must have been an element of asynchrony during the evolutionary history of the yeast genome.

The asynchrony could be a consequence of serial duplications that took place continuously over a long period of time¹². However, the organization and relative location of all the duplicated blocks in *S. cerevisiae*¹ and the chromosomal gene order in several related species¹⁶ argue against this proposal, although the occurrence of small serial duplications and deletions is likely to have a minor role during the evolution of the *Saccharomyces* yeasts^{12,13,22,23}. Another explanation for the phylogenetic asynchrony observed among the analysed genes is that different gene pairs differentiated and specialized at different time points after the genome duplication.

In our present model (Fig. 2), we propose that a whole-genome duplication took place in the progenitor of the modern *Saccharomyces* and *Kluyveromyces* yeast lineages. Assuming a constant molecular clock for the 18S ribosomal RNA upon divergence of the Ascomycota and Basidiomycota about 550 million years ago²⁴, the duplication event is estimated to have taken place about 150 million years ago. This event provided the basis for speciation of different yeast lineages and for development of new metabolic life styles, including the ability of facultative fermentation, anaerobic growth, and repression by glucose¹⁴. However, during the era that passed until both copies of any pair had evolved enough to become indispensable for the genome, most paralogous gene pairs lost one of the copies. In addition, separation of different lineages often

occurred faster than the gene-pair differentiation/specialization process (Fig. 2). We need to take into account that the acquisition of a new function of a duplicated gene boosted accumulation of mutations, especially non-synonymous ones. We imagine that the predominantly A-type genes in Table 1 are those that specialized very soon after the duplication (for example, *CIT1/2*, *PYK1/2*, *AKR1/2*, *TAL1/YGR043C* and *GUP1/2*; Table 1, Fig. 2). Predominantly B-type genes would be those that retained the same function as their duplicated partner for a longer period, and which probably regularly exchanged sequence through gene conversion (for example, *PHO87/90*, *RPS23A/B*, *BUL1/2* and *RPL13A/B*) and did not specialize until a majority of lineages had speciated. The presence of both A- and B-type genes within the same block is also a relic of the asynchronous gene specialization process.

We note that our model (Fig. 2) does not contradict the observations used as the basis for the previously presented models of single-genome duplication¹⁶ and for a series of continuous duplications¹². The ancient genome duplication, asynchronous differentiation and deletion of genes have been accompanied by several other events, like extensive micro- and macro-reorganization of the chromosomes¹³ and minor duplication events^{22,23}, which have reshaped the yeast genomes into the contemporary forms. Initially, the number of centromeres was doubled, but only the *S. cerevisiae* and *S. bayanus* lineage retained the double chromosome number; other lineages apparently lost some of the duplicated centromeres during extensive chromosome reorganizations. A whole-genome duplication followed by asynchronous differentiation/deletion events, like that proposed here, might also explain

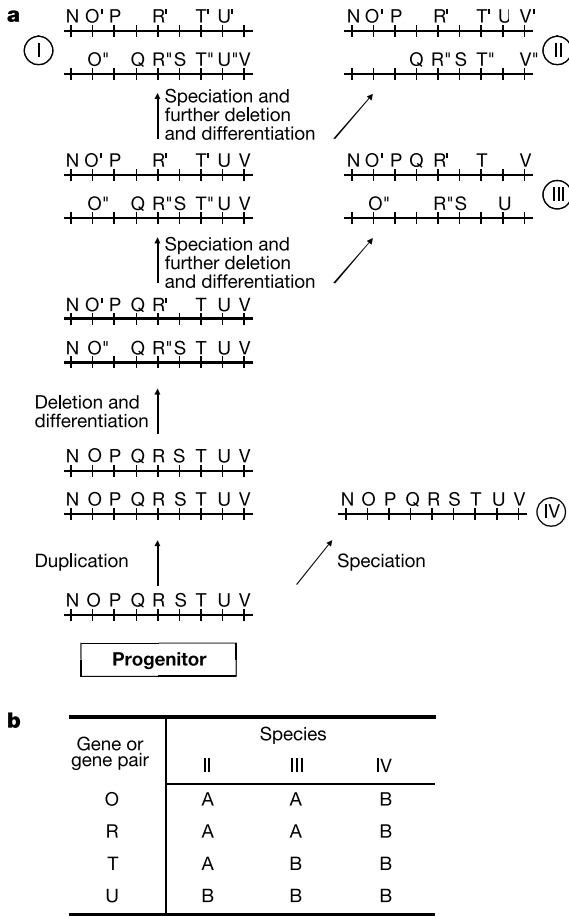


Figure 2 The origins of the modern yeast genomes. Shown are a genome duplication followed by asynchronous deletions and differentiation/specialization within the duplicated genes (a), and the phylogenetic relationship among the duplicated gene pairs of yeast I and the homologous genes from other lineages, II–IV (b). The contemporary yeasts are indicated as post-duplication lineages, I–III, and a pre-duplication lineage, IV. Single genes are designated as N–V, and the contemporary gene pairs as N'–V' and N''–V''. The differentiation/specialization of the gene pairs is accompanied by asynchronous deletions of several non-specialized genes. During these processes, different yeast lineages have branched out at different time points, resulting in the different ratios of the A- and B-type genes.

the reshaping of the genome and chromosomes of other species, including humans. □

Methods

Homologues/orthologues of the duplicated genes

Sequences of *S. bayanus* 623–6C, *S. castellii* CBS 4309, *S. kluyveri* CBS 3082 and *K. lactis* CLIB 210 genes, homologous to the *S. cerevisiae* duplicated genes¹¹, were obtained by further sequencing of the partially sequenced plasmid clones obtained from the Génolevures project¹⁵, cloning and sequencing from genomic libraries¹³, and assembly of whole-genome shotgun sequences obtained at the Genome Sequencing Center of Washington University, St Louis²⁵. *C. albicans*, *Schizosaccharomyces pombe* and other fungal sequences were obtained from GenBank and different sequencing projects. Over half of the analysed genes, originating from our project and the Génolevures sequencing project, have previously been analysed for the preservation of the ancient gene order^{12,13}. Cloned chromosome segments from different yeast species have had both ends sequenced and analysed for homology with the *S. cerevisiae* genes. If the orientation and the distance between the two genes originating from the same fragment has been preserved in both species, the pair has been considered as syntenic, and the observed situation is likely to reflect the configuration of these genes in the progenitor. Close to 100% of *S. bayanus* genes have exhibited synteny with *S. cerevisiae*, over 70% of *sensu lato* species genes, and over half of the analysed *S. kluyveri* and *K. lactis* genes^{12,13}. The detected synteny provides further evidence that a certain gene is a true orthologue in the analysed species. In the case of *C. albicans*, homologues were often obtained from the open reading frame translations (Assembly 6) obtained from the *Candida albicans* sequencing project (Stanford Genome Technology Center website at <http://www.sequence.stanford.edu/group/candida>).

Sequences obtained as hits using duplicated *S. cerevisiae* genes as queries in BLASTX searches (provided that the E values for these hits were less than 10⁻¹⁰) were further analysed. Therefore, often a couple or more sequences from a single species were included in the analysis. In the case of an ancient gene duplication, presumably taking place before the separation of the *C. albicans* and *Saccharomyces/Kluyveromyces* lineages, the whole family of duplicated *S. cerevisiae* genes was included in the analysis (for example, see the analysis of the *CIT* genes in Supplementary Information). In such cases, the gene originating from the ancient duplication always represented the outer group.

Sequence analysis

The sequences, usually the whole open reading frames of each gene, were aligned using ClustalX 1.8 (ref. 26), and BioEdit²⁷ was used for editing (details in Supplementary Information). Phylogenetic analysis, preferentially on the longest alignments, was carried out using both ClustalX 1.8 (neighbour joining (NJ) method, Poisson correction for distance estimation) and drawn using Tree View (Win32) 1.6.1 (ref. 28), and TREECON 1.3 b (based on clustering with UPGMA (unweighted pair group method using arithmetic averages) and the NJ method)²⁹. A minimum of 150 amino acids (aa) were used in alignments, with the exception of 142 aa from *ADY2/FUN34*. For genes encoding ribosomal proteins, nucleotide sequences were aligned, and in the case of *RPS16*, *RPS23* and *RPS24*, only 408, 438 and 351 nucleotides, respectively, were aligned (corresponding to 136 aa, 146 aa and 117 aa). Genes from the phylogenetic analysis, where relevant branches were supported by bootstrap values of at least 750 out of 1,000, were either designated as A or B type, or, in the case that the relevant branch was supported by values of 500–749 out of 1,000, as A* or B* type (Table 1). n.r. (not resolved) indicates cases having bootstrap values lower than 500, or when different methods gave different tree types. '-', indicates sequences not available. Further details on the phylogenetic analysis and additional observations can be found in Supplementary Information and in ref. 30.

Received 27 June 2002; accepted 3 January 2003; doi:10.1038/nature01419.

- Wolfe, K. H. & Shields, D. C. Molecular evidence for an ancient duplication of the entire yeast genome. *Nature* **387**, 708–713 (1997).
- Vision, T. J., Brown, D. G. & Tanksley, S. D. The origins of genomic duplications in *Arabidopsis*. *Science* **290**, 2114–2117 (2000).
- McLysaght, A., Hokamp, K. & Wolfe, K. H. Extensive genomic duplication during early chordate evolution. *Nature Genet.* **31**, 200–204 (2002).
- Koonin, E. V. & Galperin, M. Y. Prokaryotic genomes: the emerging paradigm of genome-based microbiology. *Curr. Opin. Genet. Dev.* **7**, 757–763 (1997).
- Rubin, G. M. *et al.* Comparative genomics of the eukaryotes. *Science* **287**, 2204–2215 (2000).
- International Human Genome Sequencing Consortium. Initial sequencing and analysis of the human genome. *Nature* **409**, 860–921 (2001).
- Ohno, S. *Evolution by Gene Duplication* (Springer, New York, 1970).
- Goffeau, A. *et al.* Life with 6000 genes. *Science* **274**, 563–567 (1996).
- Lalo, D., Stettler, S., Mariotte, S., Slonimski, P. P. & Thuriaux, P. Two yeast chromosomes are related by a fossil duplication of their centromeric regions. *C.R. Acad. Sci. III* **316**, 367–373 (1993).
- Melnick, L. & Sherman, F. The gene clusters ARC and COR on chromosomes 5 and 10, respectively, of *Saccharomyces cerevisiae* share a common ancestry. *J. Mol. Biol.* **233**, 372–388 (1993).
- Seoighe, C. & Wolfe, K. H. Updated map of duplicated regions in the yeast genome. *Gene* **238**, 253–261 (1999).
- Llorente, B. *et al.* Genomic exploration of the hemiascomycetous yeasts: 20. Evolution of gene redundancy compared to *Saccharomyces cerevisiae*. *FEBS Lett.* **487**, 122–133 (2000).
- Langkjer, R. B., Nielsen, M. L., Daugaard, P. R., Liu, W. & Piškur, J. Yeast chromosomes have been significantly reshaped during their evolutionary history. *J. Mol. Biol.* **304**, 271–288 (2000).
- Piškur, J. Origin of the duplicated regions in the yeast genomes. *Trends Genet.* **17**, 302–303 (2001).
- Souciet, J. *et al.* Genomic exploration of the hemiascomycetous yeasts: 1. A set of yeast species for molecular evolution studies. *FEBS Lett.* **487**, 3–12 (2000).
- Wong, S., Butler, G. & Wolfe, K. H. Gene order evolution and paleopolyploidy in hemiascomycete yeasts. *Proc. Natl Acad. Sci. USA* **99**, 9272–9277 (2002).
- Kurtzman, C. P. & Robnett, C. J. Identification and phylogeny of ascomycetous yeasts from analysis of nuclear large subunit (26S) ribosomal DNA partial sequences. *Antonie Van Leeuwenhoek* **73**, 331–371 (1998).
- Vaughan-Martini, A. & Martini, A. in *The Yeast. A Taxonomic Study* (eds Kurtzman, C. P. & Fell, J.) 358–371 (Elsevier Science, Amsterdam, 1998).
- Møller, K., Olsson, L. & Piškur, J. Ability for anaerobic growth is not sufficient for development of the petite phenotype in *Saccharomyces kluyveri*. *J. Bacteriol.* **183**, 2485–2489 (2001).
- Møller, K. *et al.* Aerobic glucose metabolism of *Saccharomyces kluyveri*: growth, metabolite production, and quantification of metabolic fluxes. *Biotechnol. Bioeng.* **77**, 186–193 (2002).
- Wesołowski-Louvel, M., Breunig, K. D. & Fukuhara, H. in *Nonconventional Yeasts in Biotechnology: a Handbook* (ed. Wolf, K.) 139–201 (Springer, Berlin, 1996).
- Hughes, T. R. *et al.* Widespread aneuploidy revealed by DNA microarray expression profiling. *Nature Genet.* **25**, 333–337 (2000).
- Wicksteed, B. L. *et al.* A physical comparison of chromosome III in six strains of *Saccharomyces cerevisiae*. *Yeast* **10**, 39–57 (1994).
- Berbee, M. L. & Taylor, J. W. in *The Mycota VIII: Systematics and Evolution* (eds McLaughlin, D. J., McLaughlin, E. G. & Lemke, P. A.) 229–245 (Springer, Berlin, 2001).
- Cliften, P. F. *et al.* Surveying *Saccharomyces* genomes to identify functional elements by comparative DNA sequence analysis. *Genome Res.* **11**, 1175–1186 (2001).
- Thompson, J. D., Gibson, T. J., Plewniak, F., Jeanmougin, F. & Higgins, D. G. The ClustalX windows interface: flexible strategies for multiple sequence alignment aided by quality analysis tools. *Nucleic Acids Res.* **24**, 4876–4882 (1997).
- Hall, T. A. BioEdit: a user-friendly biological sequence alignment editor and analysis program for Windows 95/98/NT. *Nucleic Acids Symp. Ser.* **41**, 95–98 (1999).
- Page, R. D. TreeView: an application to display phylogenetic trees on personal computers. *Comput. Appl. Biosci.* **12**, 357–358 (1996).
- Van de Peer, Y. & De Wachter, R. TREECON for Windows: a software package for the construction and

drawing of evolutionary trees for the Microsoft Windows environment. *Comput. Appl. Biosci.* **10**, 569–570 (1994).

30. Langkjær, R. B. *Re-modelling of the Nuclear and Mitochondrial Genomes during the Evolution of the Saccharomyces Yeasts*. Thesis, BioCentrum-DTU, Technical Univ., Denmark (2002).

Supplementary Information accompanies the paper on *Nature's* website (<http://www.nature.com/nature>).

Acknowledgements We thank the laboratories of C. Gaillardin and M. Bolotin-Fukuhara for providing *E. coli* clones containing genomic yeast DNA, which were partially sequenced by the Génolevures project. We thank K. H. Wolfe and his co-workers for sharing their manuscripts before publication. Sequencing of *Candida albicans* was accomplished with the support of the NIDR and the Burroughs Wellcome Fund. This work was partially supported by the Danish Research Council.

Competing interests statement The authors declare that they have no competing financial interests.

Correspondence and requests for materials should be addressed to J.P. (e-mail: jp@biocentrum.dtu.dk). The analysed gene sequences have the following GenBank accession numbers: AY144796–AY145050.

CD4⁺ T cells are required for secondary expansion and memory in CD8⁺ T lymphocytes

Edith M. Janssen^{*}, Edward E. Lemmens^{*}, Tom Wolfe[†], Urs Christen[†], Matthias G. von Herrath[†] & Stephen P. Schoenberger^{*}

^{*} Division of Cellular Immunology and [†] Division of Developmental Immunology, La Jolla Institute for Allergy and Immunology, 10355 Science Center Drive, San Diego, California 92121, USA

A long-standing paradox in cellular immunology concerns the conditional requirement for CD4⁺ T-helper (T_H) cells in the priming of cytotoxic CD8⁺ T lymphocyte (CTL) responses *in vivo*. Whereas CTL responses against certain viruses can be primed in the absence of CD4⁺ T cells, others, such as those mediated through 'cross-priming' by host antigen-presenting cells, are dependent on T_H cells^{1–4}. A clearer understanding of the contribution of T_H cells to CTL development has been hampered by the fact that most T_H-independent responses have been demonstrated *ex vivo* as primary cytotoxic effectors, whereas T_H-dependent responses generally require secondary *in vitro* re-stimulation for their detection. Here, we have monitored the primary and secondary responses of T_H-dependent and T_H-independent CTLs and find in both cases that CD4⁺ T cells are dispensable for primary expansion of CD8⁺ T cells and their differentiation into cytotoxic effectors. However, secondary CTL expansion (that is, a secondary response upon re-encounter with antigen) is wholly dependent on the presence of T_H cells during, but not after, priming. Our results demonstrate that T-cell help is 'programmed' into CD8⁺ T cells during priming, conferring on these cells a hallmark of immune response memory: the capacity for functional expansion on re-encounter with antigen.

After exposure to antigen *in vivo*, CD8⁺ T-cell responses proceed through an ordered sequence of developmental events. These include an initial expansion phase in which a significant number of cytotoxic effectors are generated, and a subsequent contraction phase in which about 90% of these die, leaving a stable population of memory cells able to mount a rapid secondary response to antigen⁵. Although transition through these stages was thought to be governed by the presence and eventual elimination of antigen, mounting evidence suggests that CD8⁺ T-cell development is

guided by an instructional programme that, once set into motion during priming, is executed independently^{6–9}. The role of T_H cells in initiating and promoting the programmed development of CD8⁺ T cells *in vivo* is poorly understood. Early *in vitro* studies gave rise to models in which help is mediated by paracrine cytokines produced by T_H cells¹⁰. Recent work, however, has focused on the role of CD4⁺ T cells in activating antigen-presenting cells (APCs) from an immature state in which they are unable to prime CTLs to a state in which they can do so autonomously^{3,11,12}. T_H-independent antigens such as viruses are thought to prime CTLs by achieving a functionally equivalent degree of APC activation as that produced by T_H cells, either through direct infection or provoking inflammatory host responses^{13,14}. Although this model provides a possible explanation for the conditional nature of T-cell help for CTL responses, it does not address which aspects of CD8⁺ development (for example, primary expansion, functional differentiation, or memory) are regulated by CD4⁺ T cells. We have now investigated this question for both T_H-dependent and T_H-independent CTL responses.

Immunization of C57BL/6 mice with syngeneic human adenovirus type 5 E1-transformed Tap^{-/-} mouse embryo cells (Tap^{-/-} 5E1 MECs) induces a prototypical T_H-dependent, CD8⁺ T-cell response through cross-priming¹⁵. Depletion of CD4⁺ cells before immunization blocks the development of E1B(192–200)-peptide-specific CTLs after secondary *in vitro* re-stimulation 14 days later³. To investigate whether the absence of T_H cells abrogates primary expansion, the frequency of interferon-γ (IFN-γ)⁺ effector CD8⁺ T cells was monitored directly *ex vivo* at weekly intervals after immunization of intact (wild type) or CD4-depleted mice. The

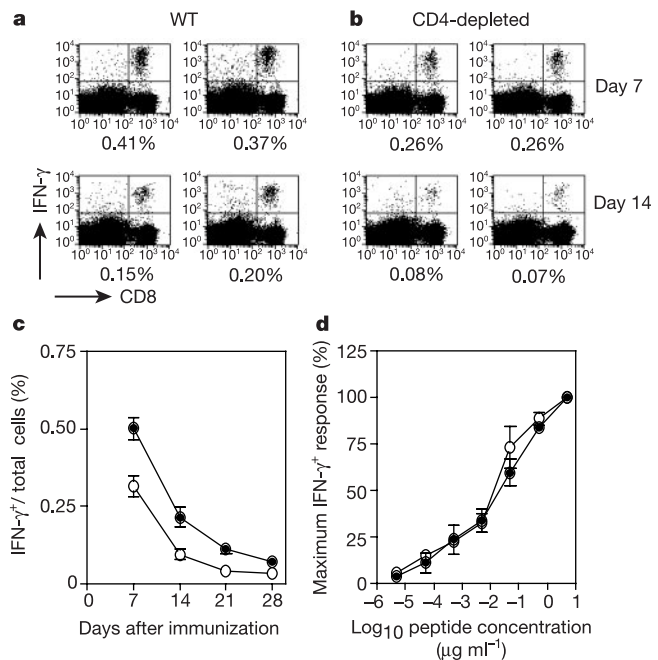


Figure 1 Functional expansion of T-helper (T_H) cell-dependent CD8⁺ T cells cross-primed in the absence of CD4⁺ T-cell help. **a, b**, The frequency of interferon-γ (IFN-γ)⁺ E1B(192–200)-specific CD8⁺ T cells detected in the spleens of Tap^{-/-} Ad5E1-immunized normal (WT) (**a**) or CD4-depleted (**b**) mice on stimulation with E1B(192–200) peptide. (Control peptide-stimulated responses were <0.01% of total splenocytes.) The value under each panel represents the percentage of total cells that are positive for IFN-γ. **c**, Percentage of IFN-γ⁺ E1B(192–200)-specific CD8⁺ cells in the spleen of normal (filled circles) and CD4-depleted (open circles) mice at various time points after immunization. **d**, Comparable functional avidity of E1B(192–200)-specific IFN-γ⁺ CD8⁺ cells of normal (filled circles) and CD4-depleted (open circles) mice after stimulation with titrated concentrations of E1B(192–200) peptide. Results are displayed as mean ± s.e.m. (*n* = 6) and are representative of three experiments.